Iran University of Science and Technology

International Journal of

Railway Research

ISSN: 2423-3838

Development of a Finite Element Methodology for Flexible Track Models in Railway Dynamics Applications

J. Pombo[1,2*], T. Almeida[1], H. Magalhães[1], P. Antunes[1], J. Ambrósio[1]

[1]IDMEC/Inst Sup Tecn, Univ Tecn Lisboa, Portugal

[2]ISEL/Inst Politecnico Lisboa, Portugal

ARTICLE INFO

Article history:
Received: 12.02.2019
Accepted: 21.04.2019
Published: 15.06.2019

Keywords:
Multibody dynamics
Finite element models
Realistic tracks
Vehicle-track interaction
Contact forces

A B S T R A C T

The dynamic analysis of railway vehicles involves the construction of three independent models: the vehicle model; the track model; and the wheel-rail contact model. In this work, a multibody formulation with Cartesian coordinates is used to describe the kinematic structure of the rigid bodies and joints that constitute the vehicle model. A methodology is also proposed in order to create detailed three-dimensional track models, which includes the flexibility of the rails and of the substructure. Here, the finite element methodology is used to model the rails as beams supported in a discrete manner by spring-damper systems that represent the flexibility of the pads, sleepers, ballast and substructure. The inclusion of flexible track models is very important to study the dynamic behavior of railway vehicles in realistic operation scenarios, especially when studying the impact of train operations on the infrastructure and, conversely, the damages on vehicles provoked by the track conditions. This topic has a significant economic impact on the vehicles maintenance and also affects the life cycle costs of tracks. The wheel-rail contact formulation used here allows obtaining, online during the dynamic analysis, the contact points location, even for the most general three-dimensional motion of the wheelsets with respect to the track. The methodology proposed to build flexible track models is validated here by comparing the results obtained with this new approach with the ones obtained with ANSYS. Furthermore, the methodology is demonstrated by studying the dynamic behavior of the Alfa Pendular railway vehicle.

1. Introduction

The railway system is increasingly becoming a key-player in worldwide transport policies. This results from the rising oil prices and from the urgency for reduction of CO2 emissions. To improve the competitiveness and attractiveness of railway networks, the trains have to travel faster, with high levels of safety and comfort, and with lower life cycle costs. Therefore, the increasing demands for network capacity, either by increasing the traffic speed or the axle loads, put pressure on the existing infrastructures and the effects of these changes have to be carefully considered. The development of computer resources led simulations to be an essential part of the design process of railway systems. The European Strategic Rail Research Agenda [1] and the European Commission White Paper for Transports [2] have identified key scientific and technological priorities for rail transport over the next 20 years. One of the points emphasized is the need to reduce the cost of approval for new vehicles and infrastructure products with the introduction of virtual certification.

*Corresponding author
Email address: jpombo@dem.ist.utl.pt

Furthermore, the use of advanced computational tools during the design phase of new trains allows carry out several simulations, under various scenarios, in order to improve its dynamic performance and reach an optimized design. In this way, studies to evaluate the impact of design changes or failure modes risks can be performed in a much faster and less costly way than the physical implementation and test of those changes in real prototypes.

Due to their multidisciplinary, all the issues involving railway systems are complex. Therefore, the use of computational tools that represent the state of the art and that are able to characterize the modern designs and predict the vehicles' performance by using validated mathematical models is essential. Recent computer codes for railway applications use specific methodologies that, in general, only allow studying each particular phenomenon at a time. By analyzing such phenomena independently, it is not possible to capture all the dynamics of the complete railway system neither the relevant coupling effects.

The main goal of this work is to develop an integrated computational tool that is able to model with detail the vehicle, the track and the subgrade. The study of these systems involves the development of complex methodologies, each requiring different mathematical formulations and numerical procedures. Here, instead of using the traditional approach, in which these systems are handled independently, they are integrated in a common and reliable tool, where the interaction among them is considered. The methodologies developed will be validated by comparison with other tools and/or in close collaboration with the railway industry using real data.

The railway vehicle considered in this study is the Alfa Pendular that is used for passenger transportation in Portugal. It is a trainset with an active tilting system which allows it to negotiate curves at speeds higher than the balanced speed [3] and keeping the non-compensated acceleration within admissible values for passenger comfort [4].

The dynamic behavior of the railway vehicle is studied using a multibody formulation [5-7] where the main structural elements are treated as rigid bodies. These are connected with flexible links that represent the suspension elements. The relative motions between the bodies of the system are restrained by using appropriate kinematic constraints. The track flexibility is included in the formulation by using finite element models [8,9] to represent the rails, which are supported by discrete elastic elements, representing the flexibility of the sleepers, pads, ballast (or slab) and subgrade. Another advantage of this methodology is that it allows building realistic track models by considering the track irregularities in the formulation [10]. These track imperfections are measured by the infrastructure managers and can be included in the track model when performing the simulations. Such feature allows assessing the consequences of the track conditions on the vehicles performance, namely noise and vibration. Furthermore, it can help scheduling the track maintenance procedures by identifying the levels of track irregularities that promote the increase of wear and/or vehicle-track interaction forces. The finite element formulation proposed here to build flexible track models is based on an analogous formulation used by the same research group to study the pantograph-catenary interaction [11, 12]. The track model pre-processor and the numerical implementation of the finite element methodology are validated here by comparing the results with the ones obtained from ANSYS. A generic wheel-rail contact detection formulation [13, 14] is applied here in order to determine, online during the dynamic analysis, the contact points location, without need to use pre-computed lookup tables. This computational efficient methodology uses an elastic force model that allows computing the normal contact forces in the wheel-rail interface, accounting for the energy loss during contact [15, 16]. The tangential wheel-rail contact forces can be calculated using one of the creep force models implemented here and described in the literature, namely the Kalker linear theory [17], Heuristic nonlinear method [18] and the Polach formulation [19]. The methodologies described in this work are applied to study the dynamic behavior of the Alfa Pendular railway vehicle, which is operated by the Portuguese Rail company in the intercity service. Future developments are directed towards studies involving the influence of the track settlement conditions on vehicles performance and analyses associated to railway infrastructure degradation resulting from trainsets operation. It is intended to assess the accuracy and suitability of the proposed methodologies through the comparison of the dynamic analysis results against those

obtained by experimental testing. For this purpose, a partnership between this research group and the Portuguese railroad company has been established.

2. Description of the Railway Vehicle

In this section, the Alfa Pendular trainset is described. This railway vehicle is used for passenger transportation in Portugal. It is a trainset with an active tilting system which allows it to negotiate curves at higher speeds, maintaining the passengers comfort within admissible values. The trainset is composed of six vehicles, being four motor units and two trailer, as shown in Figure 1.

In the following, all mechanical elements that are relevant to build the multibody model, namely the structural and the suspension elements, are described. Due to the trainset configuration, it is assumed that, concerning the studies performed here, the dynamic behavior of each vehicle has a non-significant influence on the others. According to this assumption, each vehicle of the trainset can be studied independently. In this way, the vehicle model considered here is composed only by one trailer unit of the trainset. It should be noticed that the methodology now described is generic and can be applied to any railway vehicle.

The Alfa Pendular trailer vehicle is composed by a carbody, where the passengers travel. The carbody is supported by two bogies through a set of mechanical elements that constitute the secondary suspension. The main function of these elements is to minimize the vibrations, resulting from the vehicle-track interaction, transmitted to the passenger compartment, improving the comfort and reducing the problems associated to the structural fatigue. Each bogie includes the wheelsets, which are in contact with the rails, and another group of mechanical elements that constitute the primary suspension. These elements are the main responsible for the steering capabilities and stability behavior of the whole group being, ultimately, responsible for the critical speed of the vehicle. The structural elements that compose the Alfa Pendular vehicle are represented in Figure 2(a), namely the carbody, bogie frame, wheelset and the axlebox. The primary suspension of the vehicle at each

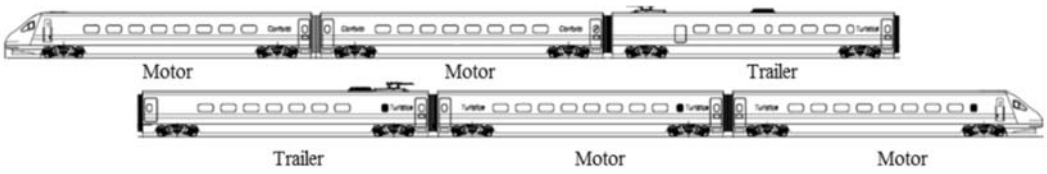

Figure 1. Schematic representation of the Alfa Pendular trainset

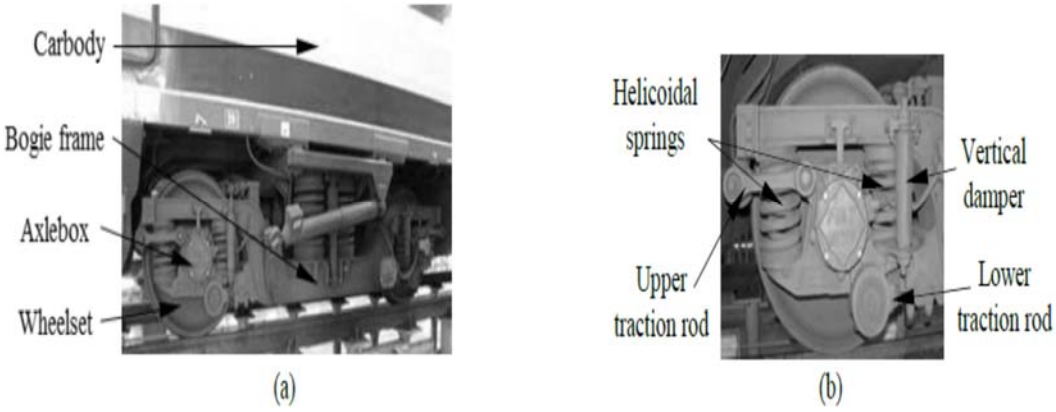

Figure 2. Alfa Pendular vehicle: (a) Structural elements; (b) Primary suspension elements

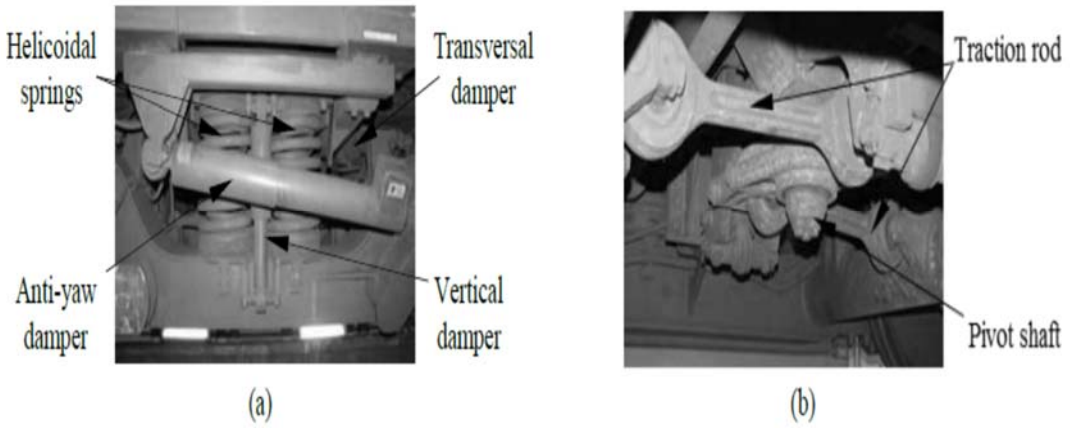

Figure 3. Alfa Pendular vehicle: (a) Secondary suspension elements; (b) Bogie-carbody connection elements

axlebox, shown in Figure 2(b), is composed by two helicoidal springs, one vertical damper and one upper and lower traction rods. The secondary suspension elements are shown in Figure 3(a). In each side of the bogie, this subsystem is composed by two helicoidal springs, one vertical damper, one transversal damper and one anti-yaw damper. The carbody is connected to the bogie through a pivot shaft, which is rigidly fixed to the carbody, as depicted in Figure 3(b). The pivot is assembled vertically and it is connected to the bogie frame by two traction rods, which allow the relative motion between these structural elements.

building each subsystem independently, being the whole vehicle model build by assembling the subsystems as they were Lego pieces. The subsystems considered here to model the Alfa Pendular vehicle are shown in Figure 4.

The subsystem 0 is used to represent the track and the infrastructure, as shown in Figure 5(a). The subsystem 1, depicted in Figure 5(b), represents the carbody of the vehicle. The subsystems 2 and 3, shown in Figure 5(c), represent the front and the rear bogies. Being these last two equal, it is only necessary to build one subsystem representing the bogie. Then, when assembling the railway vehicle, this subsystem is used twice to represent both the

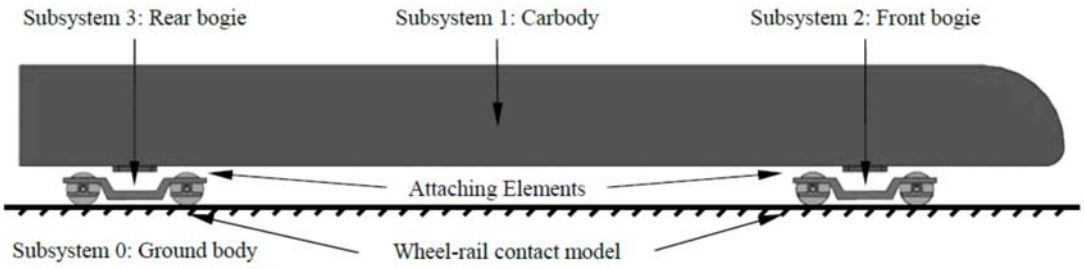

Figure 4. Alfa Pendular multibody model

3. Description of the Vehicle Multibody Model

The first step for modeling the railway vehicle using a multibody formulation is the division of the group in several subsystems, which are simpler to handle. This strategy allows

front and the rear bogies. The subsystem 1 is connected to subsystems 2 and 3 by attaching elements, which represent the secondary suspension and the bogie-carbody connection elements. The interaction between the rails (from subsystem 0) and the wheels (from subsystems 2

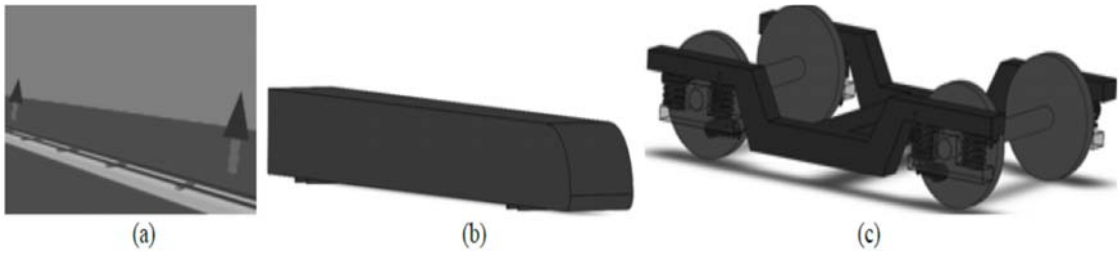

Figure 5. Subsystems of multibody model: (a) Track and infrastructure; (b) Carbody; (c) Front and rear bogies

and 3) is performed by using an appropriate wheel-rail contact model [13, 14].

For each subsystem it is necessary to provide the information about the rigid bodies, kinematic joints and linear and/or nonlinear force elements. The data for the definition of the rigid bodies includes the mass, the inertia properties and the initial position and orientation. The position of each body is measured from the origin of subsystem reference frame to the center of mass of the body. The relative motion between the bodies is limited by kinematic joints [5], which restrain relative degrees-of-freedom between the bodies connected by them.

The suspension components, such as springs and dampers that connect the rigid bodies, are modeled as force elements. These are responsible for transmitting the internal forces that are developed in the system as function of the relative motion among the bodies. The data required to model the suspension elements includes the coordinates of the attaching points and their stiffness and damping properties. All the data required to model the Alfa Pendular vehicle is obtained from technical information provided by the manufacturer and by the railway operator.

The subsystem 1 is defined by one body, the carbody, which is free of any constraint. Its connection to the bogies is made by the secondary suspension elements when assembling the whole system. Subsystems 2 and 3, representing the bogies, are composed by one bogie frame, four axleboxes and two wheelsets. The relative motion between the wheelsets and the axleboxes is limited by revolute joints, representing the roller bearings of the axleboxes.

The primary suspension elements are used to connect the bogie frame to the axleboxes. The helicoidal springs, shown in Figure 2(b), despite being assembled vertically, originate forces in the three directions. Therefore, they are modeled here by using linear force elements in the vertical, longitudinal and lateral directions, as represented in Figure 6(a). The vertical damper is modeled as is shown in Figure 6(b).

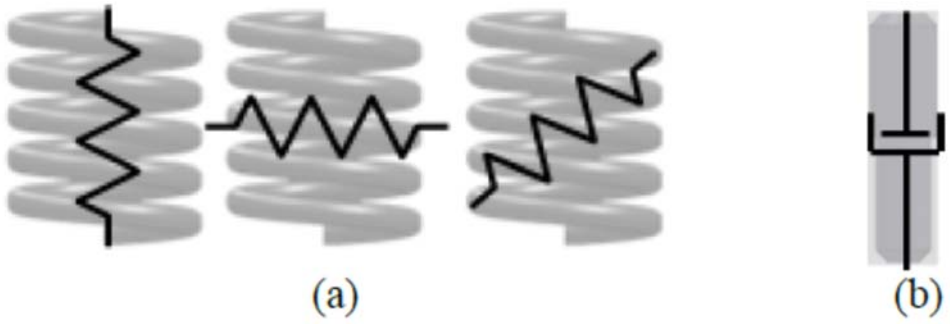

Figure 6. Primary suspension model: (a) Helicoidal spring; (b) Vertical damper

The upper and lower traction rods have equal mechanical properties, being assembled with rubber bushings at their extremities, which allow small misalignments in the lateral direction. Hence, the traction rods are modeled here as springs with different stiffness characteristics in

Figure 7. Traction rod model: (a) Longitudinal direction; (b) Lateral direction

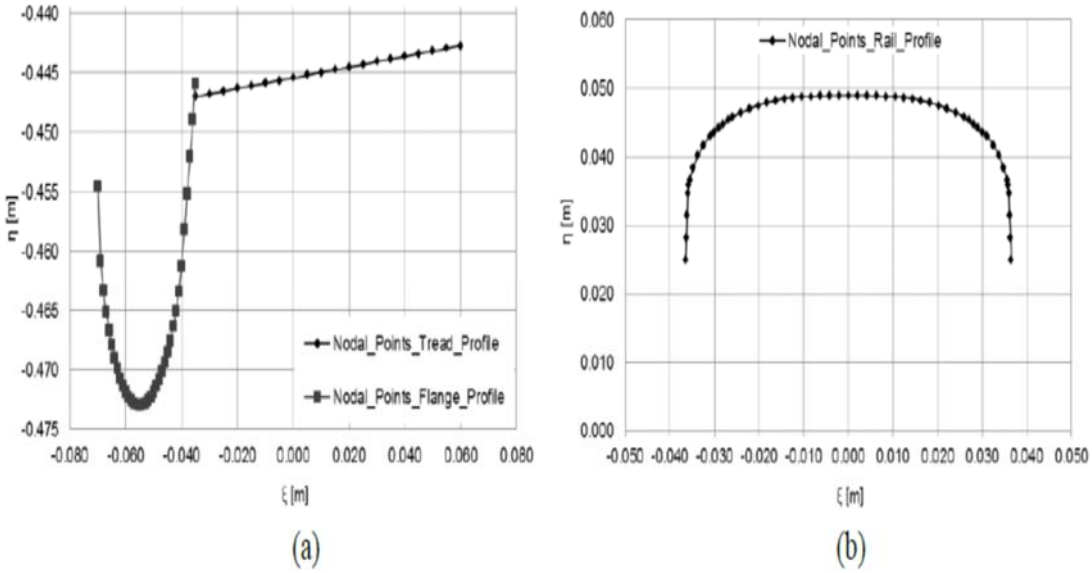

Figure 8. Nodal points representing the: (a) Wheel profile; (b) Rail profile

the longitudinal and lateral directions, as represented in Figure 7.

The longitudinal stiffness coefficient of the traction rod is obtained by the association in series between two springs, representing the rubber bushings, and another spring, representing the traction rod itself.

The wheel-rail contact formulation requires the accurate definition of the contacting geometries. This is done here by providing a set of control points that are representative of the wheel and rail profiles as shown in Figure 8. Then, during the dynamic analysis, the computational tool calculates the location of the contact points and, using appropriate methodologies, computes the normal and tangential contact forces. The detailed description of the formulation used here to study the wheel-rail contact phenomena is outside the scope of this text. The interested reader is referred to the works [13, 14].

After building all subsystems, they need to be assembled. The first step is to define the location of each subsystem with respect to the global reference frame (x,y,z), as shown in Figure 9. Then, subsystem 1 is attached to subsystems 2 and 3 by using the secondary suspension and the bogie-carbody connection elements. This is done using the same approach as the one used to assemble the primary suspension elements of the bogie subsystem.

4. Description of the Railway Track

A railway track is generally composed by an assembly of elements of distinct elasticity

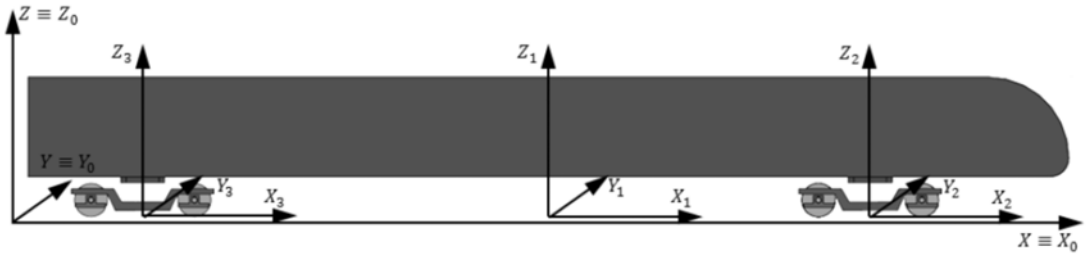

Figure 9. Subsystems assemblage

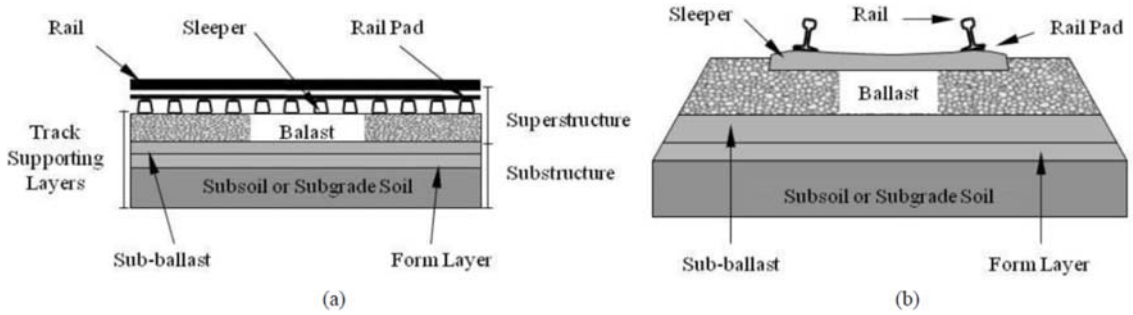

Figure 10. Main components of the railway track (a) Longitudinal view; (b) Cross-section view

responsible for gradually transmitting to the subsoil the dynamic loadings arising from the trains' passage, besides the important function of guiding the vehicles. These elements are the rails, which are supported by the sleepers through the pads. The sleepers rest on an elastic bed made up of supporting layers as ballast, subballast, formlayer and subsoil, as represented in Figure 10.

5. Overview of the Finite Element Formulation

Despite being considered as rigid by many authors and computational tools, the railway track exhibits some flexibility that is characterized by small deformations and rotations, which, besides other phenomena, originate track irregularities. Due to its nature and magnitude, these deformations can be characterized as linear. In this work the railway track system is modeled with linear finite elements, being the wheel-rail contact forces included in the force vector of the finite element formulation. The rails and sleepers are modeled by using Euler-Bernoulli beam elements, while the foundations and rail pads are represented by spring-damper elements acting in the six degrees of freedom, as shown in Figure 11. Following this approach, the equilibrium equations of the finite element method for the railway track structural system are assembled as:

$$\boldsymbol{Ma} + \boldsymbol{Cv} + \boldsymbol{Kd} = \boldsymbol{f} \tag{1}$$

where **M**, **C** and **K** are the finite element global mass, damping and stiffness matrices of the finite element model of the track. Proportional damping is used to evaluate the global damping matrix, i.e. $\mathbf{C} = \alpha\,\mathbf{K} + \beta\,\mathbf{M}$ with α and β being suitable proportionality factors [20]. Alternatively a local damping matrix can be evaluated for each finite element, i.e. $\mathbf{C}^e = \alpha^e\,\mathbf{K}^e + \beta^e\,\mathbf{M}^e$ with α^e and β^e being proportionality factors associated with each type of track element, such as the rail or sleeper; with the exception of the spring-damper elements, which have their own damping coefficients in each degree of freedom. The nodal displacements vector is expressed by **d**, while **v** is the vector of nodal velocities, **a** is the vector of nodal accelerations and **f** is the force vector, written as:

$$\boldsymbol{f} = \boldsymbol{f}_{(g)} + \boldsymbol{f}_{(c)} \tag{2}$$

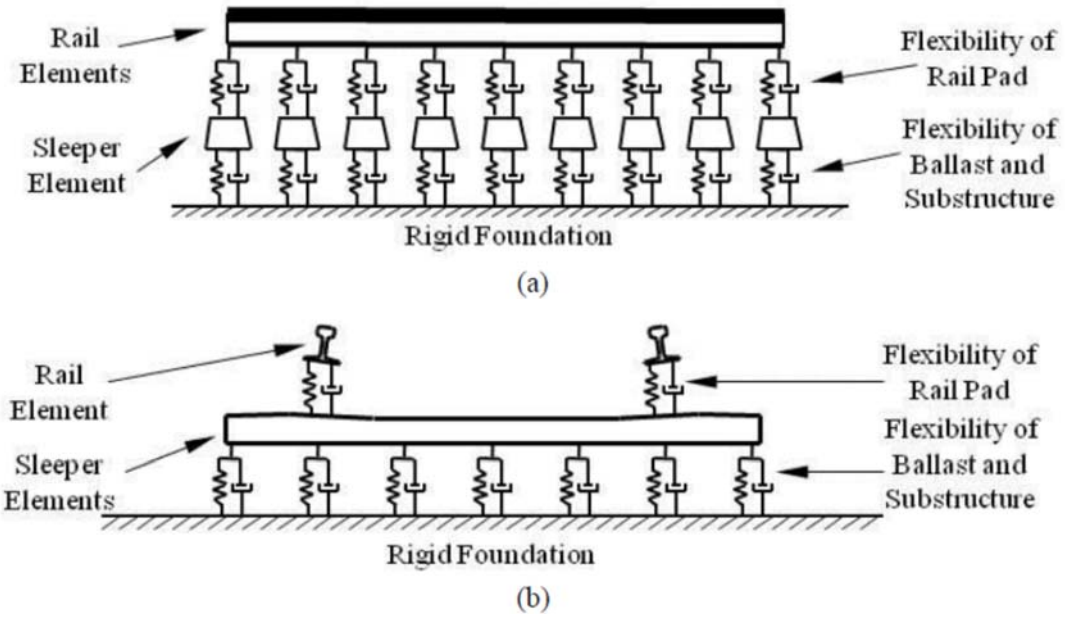

Figure 11. Main components of the track model: (a) Longitudinal view; (b) Cross-section view

which contains the gravity forces, $\mathbf{f}_{(g)}$, plus the wheel-rail contact forces, $\mathbf{f}_{(c)}$, that are developed at each time step.

In this work, the integration of the nodal accelerations uses a Newmark family integration algorithm [21]. The contact forces are evaluated for $t+\Delta t$ based on the position and velocity predictions of the finite element (FE) mesh and of the vehicle model. The finite element mesh accelerations are calculated by:

$$(\boldsymbol{M} + \gamma\Delta t\boldsymbol{C} + \beta\Delta t^2\boldsymbol{K})\boldsymbol{a}_{t+\Delta t} = \boldsymbol{f}_{t+\Delta t} - \boldsymbol{C}\widetilde{\boldsymbol{V}}_{t+\Delta t} - \boldsymbol{K}\widetilde{\boldsymbol{d}}_{t+\Delta t} \quad (3)$$

According with this approach, predictions for new positions and velocities of the nodal coordinates of the linear finite element model of the track are computed as:

$$\widetilde{\boldsymbol{d}}_{t+\Delta t} = \boldsymbol{d}_t + \Delta t\,\boldsymbol{V}_t + \frac{\Delta t^2}{2}(1-2\beta)\boldsymbol{a}_t \quad (4)$$

$$\widetilde{\boldsymbol{V}}_{t+\Delta t} = \boldsymbol{V}_t + \Delta t(1-\gamma)\boldsymbol{a}_t \quad (5)$$

Then, knowing the accelerations $\mathbf{a}_{t+\Delta t}$, the positions and velocities of the finite element mesh at next time step $t+\Delta t$ are corrected by:

$$\boldsymbol{d}_{t+\Delta t} = \widetilde{\boldsymbol{d}}_{t+\Delta t} + \beta\Delta t^2\boldsymbol{a}_{t+\Delta t} \quad (6)$$

$$\boldsymbol{V}_{t+\Delta t} = \widetilde{\boldsymbol{V}}_{t+\Delta t} + \gamma\Delta t\boldsymbol{a}_{t+\Delta t} \quad (7)$$

This correction procedure, expressed by using equations (4) through (7) and solving equation (3), is repeated until convergence is reached for a given time step, i.e. until $\left|\boldsymbol{d}_{t+\Delta t} - \widetilde{\boldsymbol{d}}_{t+\Delta t}\right| < \varepsilon_d$ and $\left|\boldsymbol{V}_{t+\Delta t} - \widetilde{\boldsymbol{V}}_{t+\Delta t}\right| < \varepsilon_v$, ε_d and ε_v being user defined tolerances.

6. Description of the Flexible Track Model

In the following, the data required to define the flexible track model is described together with the pre-processor developed to build its FE mesh. In order to define a given railway track, it is necessary to provide information about the geometry of each rail. This is done in 3D space by defining a set of control points that are representative of the geometry of each rail. In addition, it is necessary to provide the Cartesian components of the tangential **t**, normal **n** and binormal **b** vectors that define the rail referential associated to each nodal point. These quantities are tabulated as function of the rail arc length, as represented in Table 1.

After defining the 3D geometry of each rail, it is necessary to provide information about the number of track segments to be considered in the finite element mesh. For each segment, it is necessary to define its name, length and the refinement level of the mesh, as represented in Table 2.

For each track segment defined in Table 2, it is necessary to provide information about the

Table 1. Rail geometry data

Rail arc Length	X_i	Y_i	Z_i	Tx_i	Ty_i	Tz_i	Nx_i	Ny_i	Nz_i	Bx_i	By_i	Bz_i
<No.>	<No.>	<No.>	<No.>	<No.>	<No.>	<No.>	<No.>	<No.>	<No.>	<No.>	<No.>	<No.>
…	…	…	…	…	…	…	…	…	…	…	…	…
<No.>	<No.>	<No.>	<No.>	<No.>	<No.>	<No.>	<No.>	<No.>	<No.>	<No.>	<No.>	<No.>

Table 2. Track segments data

Number of Track Types	<No.>		
Track Type i	Track Type Name	Length of Track Type i	Refinement Level of Track Type i
Track Type 1	<Track Type 1 Name>	<No.>	<No.>
Track Type 2	<Track Type 2 Name>	<No.>	<No.>
…	…	…	…
Track Type n	<Track Type n Name>	<No.>	<No.>

Table 3. Track segment components data

Track Type n	<Track Type n Name>
Rail data Type	<Rail Data Type Name>
Sleepers Data Type	<Sleepers Data Type Name>
Foundations Data Type	<Foundations Data Type Name>

types of rails, sleepers and foundations that compose each one, as represented in Table 3.

Then, for each rail, it is necessary to define the properties required for the Euler-Bernoulli beam elements formulation, as represented in Table 4.

After introducing the information about the rails, it is necessary to provide all properties required to define the sleepers for each track segment, as represented in Table 5.

Besides the information about the rails and sleepers, the properties for the definition of the foundations for each track segment are required, as represented in Table 6.

As previously referred, the rails and sleepers are modeled by using Euler-Bernoulli beam elements. For this purpose, it is necessary to define their geometry. The rail geometry data is provided in Table 4. For the sleepers, with a general geometry shown in Figure 12, the data

Table 4. Rail geometry data

Rail Data Type	<Rail Data Type n Name>
UIC Rail Code	<Code>
Young Modulus - E [Pa]	<No.>
Poisson Coefficient	<No.>
Cross Section Area [m^2]	<No.>
Second Moment of Area in xz Plane - Iyy [m^4]	<No.>
Second Moment of Area in xy Plane - Izz [m^4]	<No.>
Second Moment of Area in yz Plane - Ixx [m^4]	<No.>
Density [kg/m^3]	<No.>
Torsion Modulus - G [Pa]	<No.>
Rayleigh Damping Parameter α	<No.>
Rayleigh Damping Parameter β	<No.>

Table 5. Sleeper properties data

Sleepers Data Type	<Sleepers Data Type n Name>
Sleepers Distance [m]	<No.>
Number of Nodes Between Sleepers	<No.>
Sleeper Geometry	Sleeper Geometry Name
Pad Longitudinal Stiffness Kx [N/m]	<No.>
Pad Transversal Stiffness Ky [N/m]	<No.>
Pad Vertical Stiffness Kz [N/m]	<No.>
Pad Vertical Rotational Stiffness Kry [N/m]	<No.>
Pad Transversal Rotational Stiffness Krz [N/m]	<No.>
Pad Torsion Stiffness Kt [N/m]	<No.>
Pad Longitudinal Damping Cx [N.s/m]	<No.>
Pad Transversal Damping Cy [N.s/m]	<No.>
Pad Vertical Damping Cz [N.s/m]	<No.>
Pad Vertical Rotational Damping Cry [N.s/m]	<No.>
Pad Transversal Rotational Damping Crz [N.s/m]	<No.>
Pad Torsion Damping Ct [N.s/m]	<No.>

required to define their geometry is represented in Table 7.

Finally it is necessary to define the constants and output parameters for the track model. These quantities are represented in Table 8.

7. Validation of the Flexible Track Methodology

In order to validate the methodology proposed here, a realistic flexible track model is built and subjected to loads representing the wheelset of a railway vehicle, as depicted in

Table 6. Foundation properties data

Foundations Data Type	<Foundations Data Type n Name>
Longitudinal Stiffness Kx [N/m]	<No.>
Transversal Stiffness Ky [N/m]	<No.>
Vertical Stiffness Kz [N/m]	<No.>
Vertical Rotational Stiffness Kry [N/m]	<No.>
Transversal Rotational Stiffness Krz [N/m]	<No.>
Torsion Stiffness Kt [N/m]	<No.>
Longitudinal Damping Cx [N.s/m]	<No.>
Transversal Damping Cy [N.s/m]	<No.>
Vertical Damping Cz [N.s/m]	<No.>
Vertical Rotational Damping Cry [N.s/m]	<No.>
Transversal Rotational Damping Crz [N.s/m]	<No.>
Torsion Damping Ct [N.s/m]	<No.>

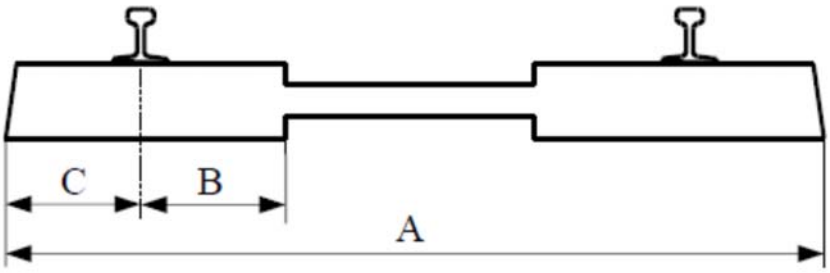

Figure 12. Sleeper general geometry

Table 8. Track model constants and output parameters

Track Constants		Output Parameters	
Gravity Acceleration [m/s^2]:	<No.>	Deformation Scalar Factor:	<No.>

Figure 13. The results obtained are compared against the ones provided by ANSYS 12. The data used to build the flexible track model is given in Table 9 through Table 12.

In this case study, a pair of static downward vertical forces P of 112.5 kN are applied, as depicted in Figure 13(b). These forces represent the maximum wheelset load of 22.5 ton that a railway vehicle can have to be allowed to operate in the Portuguese railway network. In ANSYS, the BEAM4 element was used, corresponding to an Euler-Bernoulli beam element. All the other parameters required to build the track model in ANSYS match the ones used by the computational tool proposed here.

The deformations obtained with the two numerical tools are shown in Figure 14 and Figure 15. As the deformations are very small when compared with the other dimensions of the track, they are incremented by a factor of 100 in

Table 7. Sleeper geometry data

Sleeper Geometry	<Sleeper Geometry n Name>
Sleeper Length (Parameter A) [m]	<No.>
Rail-to-End Position (Parameter C) [m]	<No.>
Rail-to-Start Position (Parameter B) [m]	<No.>
End Young Modulus - E [Pa]	<No.>
End Poisson Coefficient	<No.>
End Cross Section Area [m^2]	<No.>
End Second Moment of Area in xz Plane - Iyy [m^4]	<No.>
End Second Moment of Area in xy Plane - Izz [m^4]	<No.>
End Second Moment of Area in yz Plane - Ixx [m^4]	<No.>
End Density [kg/m^3]	<No.>
End Torsion Modulus - G [Pa]	<No.>
End Rayleigh Damping Parameter α	<No.>
End Rayleigh Damping Parameter β	<No.>
Start Young Modulus - E [Pa]	<No.>
Start Poisson Coefficient	<No.>
Start Cross Section Area [m^2]	<No.>
Start Second Moment of Area in xz Plane - Iyy [m^4]	<No.>
Start Second Moment of Area in xy Plane - Izz [m^4]	<No.>
Start Second Moment of Area in yz Plane - Ixx [m^4]	<No.>
Start Density [kg/m^3]	<No.>
Start Torsion Modulus - G [Pa]	<No.>
Start Rayleigh Damping Parameter α	<No.>
Start Rayleigh Damping Parameter β	<No.>
Middle Young Modulus - E [Pa]	<No.>
Middle Poisson Coefficient	<No.>
Middle Cross Section Area [m^2]	<No.>
Middle Second Moment of Area in xz Plane - Iyy [m^4]	<No.>
Middle Second Moment of Area in xy Plane - Izz [m^4]	<No.>
Middle Second Moment of Area in yz Plane - Ixx [m^4]	<No.>
Middle Density [kg/m^3]	<No.>
Middle Torsion Modulus - G [Pa]	<No.>
Start Rayleigh Damping Parameter α	<No.>
Start Rayleigh Damping Parameter β	<No.>

these figures. The results obtained show that the maximum vertical deformation of the track is 2.7 mm. On the other hand, in the longitudinal and lateral directions, the maximum displacement of the nodes where the forces are applied is 7.1×10^{-6} m and 32.7×10^{-6} m, respectively.

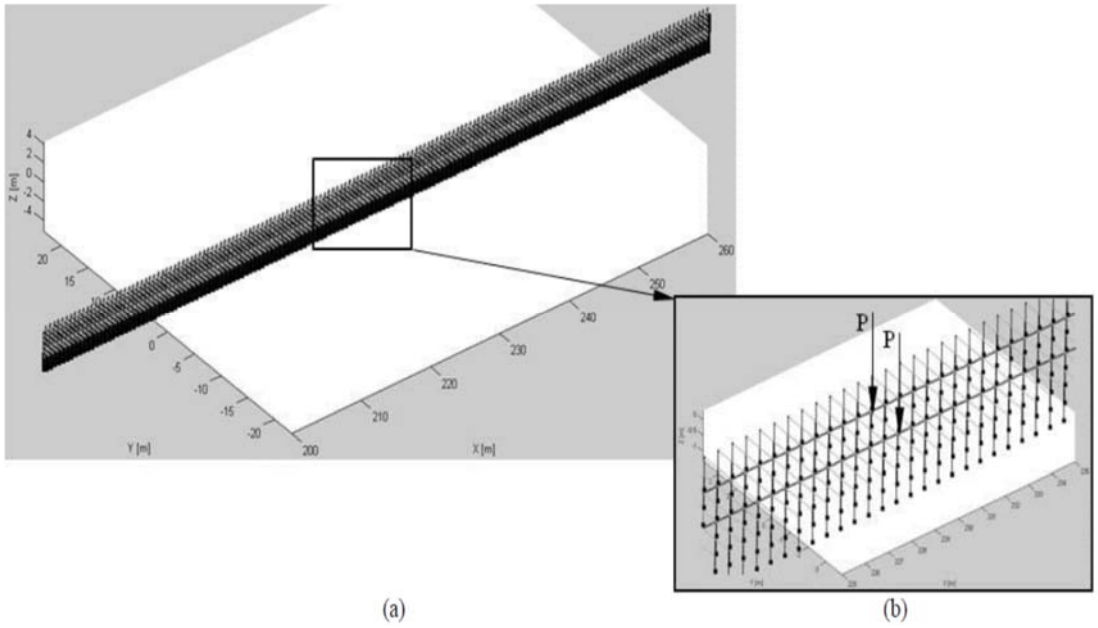

Figure 13. Flexible track model: (a) Finite element mesh; (b) External loads applied

Table 9. Track segments data for the case study

Number of Track Types	1		
Track Type i	Track Type Name	Length of Track Type i	Refinement Lev el of Track Type i
Track Type 1	Track1	500	1

When comparing the results obtained with the methodology proposed here and with ANSYS, it is observed that the maximum relative error for the track vertical deformation is about 0.04%, as shown in Figure 16, corresponding to a maximum absolute error of 1.3×10^{-7} m. Notice that the 0% error corresponds to the constrained nodes.

Figure 17(a) presents the relative errors on the rail nodes that are in the vicinity of the ones where vertical wheelset forces were applied. The relative error for the track vertical deformation on the nodes of the sleeper subjected to the external loads is shown in Figure 17(b). These results allow concluding that the finite element methodology proposed here to represent the track flexibility is suitable for such studies and it is quantitatively validated.

8. Communication between Multibody and Finite Element Codes

In this work, a fully 3D methodology to study the interaction of a railway vehicle, described by a multibody formulation, with a flexible track, represented by a finite element methodology, is proposed. Instead of using the conventional approach, in which the vehicle dynamics, the track and subgrade are handled independently, here an integrated strategy is proposed to handle the vehicle-track-subgrade coupled dynamics. For this purpose, a high-speed co-simulation procedure is setup in order to establish a communication protocol between the multibody and the finite element codes. The vehicle-track interaction forces are computed by using an appropriate wheel-rail contact formulation [13, 14]. For the dynamic analysis of the finite

Table 10. Rail and sleeper data for the case study

Rail Data Type	UIC60	Sleepers Data Type	Sleeper1
UIC Rail Code	UIC60	Sleepers Distance [m]	0.6
Young Modulus - E [Pa]	200×10^{9}	Number of Nodes Between Sleepers	5
Poisson Coefficient	0.29	Sleeper Geometry	A
Cross Section Area [m^2]	7.68600×10^{-3}	Pad Traction Stiffness K [N/m]	85×10^{6}
Second Moment of Area in xz Plane - Iyy [m^4]	0.03055×10^{-3}	Pad Rotational Stiffness K [N/m]	8500×10^{6}
Second Moment of Area in xy Plane - Izz [m^4]	0.00513×10^{-3}	Pad Torsional Stiffness K [N/m]	8500×10^{6}
Second Moment of Area in yz Plane - Ixx [m^4]	0.04240×10^{-3}	Pad Traction Damping C [N.s/m]	85×10^{6}
Density [kg/m^3]	7.80600×10^{-3}	Pad Rotational Damping C [N.s/m]	8500×10^{6}
Torsion Modulus - G [Pa]	79.30000×10^{9}	Pad Torsional Damping C [N.s/m]	8500×10^{6}
Rayleigh Damping Parameter α	0.6		
Rayleigh Damping Parameter β	0.1		

elements model, a Newmark family numerical integrator [21] using a fixed time step is used, while for the multibody vehicle model the integration procedure is based on a predictor-corrector algorithm with variable time step [22]. The compatibility between the two integration algorithms, for the implementation of the co-simulation environment, imposes that the state variables of the two sub-systems are readily available during the integration time and also that a reliable prediction of the contact forces is available at any given time step.

One of the most critical issues of using co-simulation procedures is the added computational cost due to data exchange between codes, especially when this data is large or, as is this case, it is accessed frequently. The time spent on data exchange between applications must be negligible compared to the computation time costs of the two analyses. The use of physical data files for information exchange, also known as file input/output, is a robust, well known and very popular methodology. However, for either a recursive use or for large data sets it leads to slow data exchange when compared to the use of virtual memory sharing. In order to address this, the memory sharing process adopted on this work is done via memory mapped files.

9. Preliminary Results

In the following, the interaction between the Alfa Pendular railway vehicle and the track is analyzed. The simulation scenario corresponds to a straight track, without irregularities, and a velocity of 90 km/h. At the initial time of analysis the vehicle is assembled in the track with a lateral misalignment of 2 mm. The lateral displacement of the vehicle wheelsets is shown in Figure 18. It is observed that, after the initial misalignment of 2 mm, the hunting motion of the wheelsets is damped and they return to the center position on the track. These results show that the critical speed [3] of the vehicle is higher than 90 km/h.

Table 11. Foundation properties for the case study

Foundations Data Type	Foundation 1
Foundation Traction Stiffness K [N/m]	4783539
Foundation Rotational Stiffness K [N/m]	478353900
Foundation Torsional Stiffness K [N/m]	478353900
Foundation Traction Damping C [N.s/m]	4783539
Foundation Rotational Damping C [N.s/m]	478353900
Foundation Torsional Damping C [N.s/m]	478353900

Table 12. Sleeper geometry for the case study

Sleeper Geometry	A
Sleeper Length (Parameter A) [m]	2.250
Rail-to-End Position (Parameter C) [m]	0.372
Rail-to-Start Position (Parameter B) [m]	0.378
End Young Modulus - E [Pa]	65×10^{9}
End Poisson Coefficient	0.15
End Cross Section Area [m^2]	70.3030×10^{-3}
End Second Moment of Area in xz Plane - Iyy [m^4]	0.9824×10^{-3}
End Second Moment of Area in xy Plane - Izz [m^4]	1.3170×10^{-3}
End Second Moment of Area in yz Plane - Ixx [m^4]	0.3723×10^{-3}
End Density [kg/m^3]	2.4×10^{3}
End Shear Modulus - G [Pa]	2.4×10^{9}
Start Young Modulus - E [Pa]	65×10^{9}
Start Poisson Coefficient	0.15
Start Cross Section Area [m^2]	70.3030×10^{-3}
Start Second Moment of Area in xz Plane - Iyy [m^4]	0.9824×10^{-3}
Start Second Moment of Area in xy Plane - Izz [m^4]	1.3170×10^{-3}
Start Second Moment of Area in yz Plane - Ixx [m^4]	0.3723×10^{-3}
Start Density [kg/m^3]	2.4×10^{3}
Start Shear Modulus - G [Pa]	2.4×10^{9}
Middle Young Modulus - E [Pa]	65×10^{9}
Middle Poisson Coefficient	0.15
Middle Cross Section Area [m^2]	70.3030×10^{-3}
Middle Second Moment of Area in xz Plane - Iyy [m^4]	64.4063×10^{-3}
Middle Second Moment of Area in xy Plane - Izz [m^4]	86.3438×10^{-3}
Middle Second Moment of Area in yz Plane - Ixx [m^4]	0.3723×10^{-3}
Middle Density [kg/m^3]	2.4×10^{3}
Middle Shear Modulus - G [Pa]	2.2×10^{9}

The lateral and vertical contact forces on the left wheels of the Alfa Pendular vehicle are shown in Figure 19 and Figure 20, respectively. The results show that the forces oscillations decrease as the vehicle returns to the center position on the track after the initial misalignment. Notice that the first second of dynamic analysis was not considered as they represent the transient phase of the contact forces.

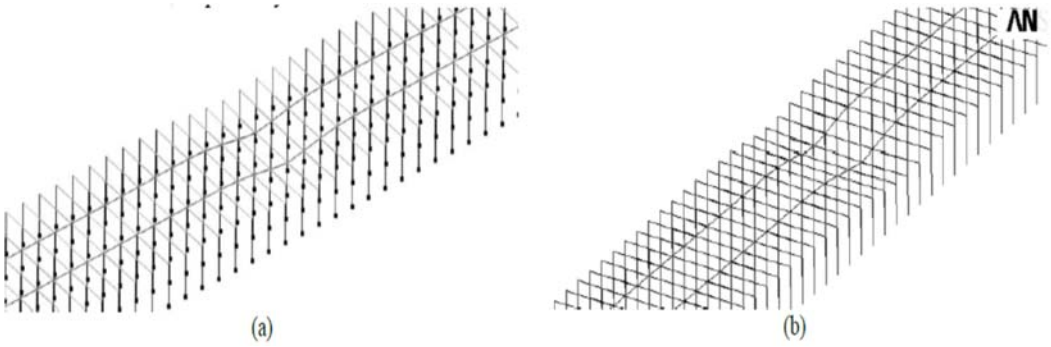

Figure 14. Perspective view of the track deformation (deformation scaled × 100): (a) Computational tool; (b) ANSYS

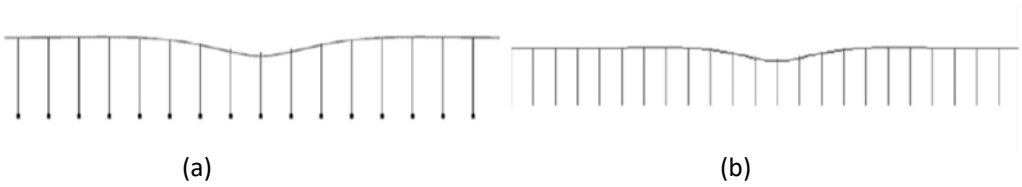

Figure 15. Lateral view of the track deformation (deformation scaled × 100): (a) Computational tool; (b) ANSYS

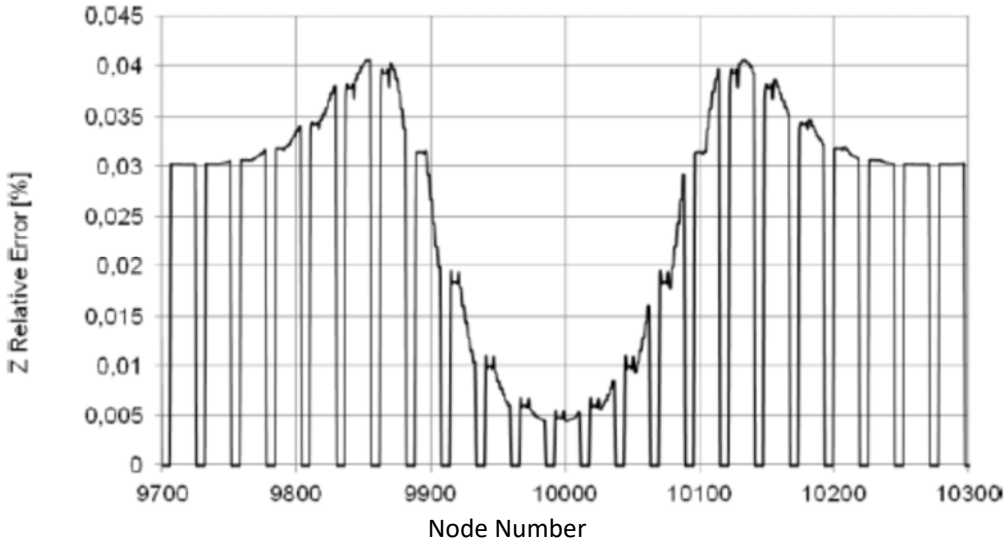

Figure 16. Relative error for the track vertical deformation

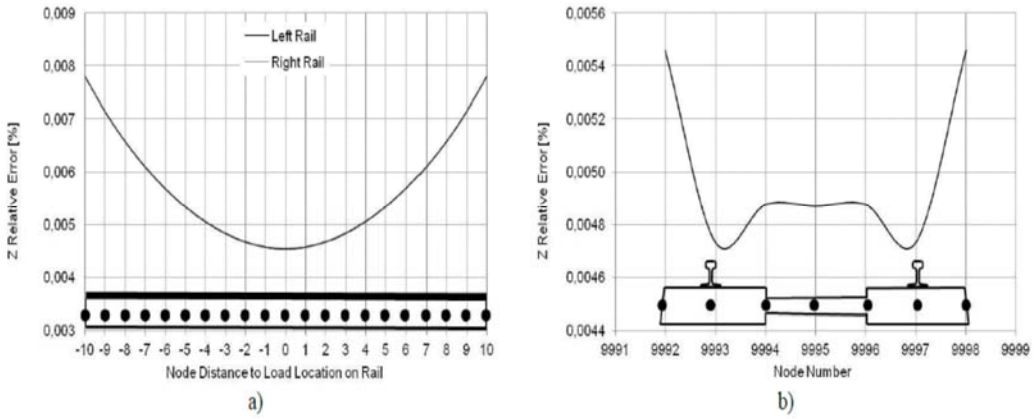

Figure 17. Relative error on the nodes in the vicinity of the applied loads: (a) Nodes on the rail; (b) Nodes on the sleeper

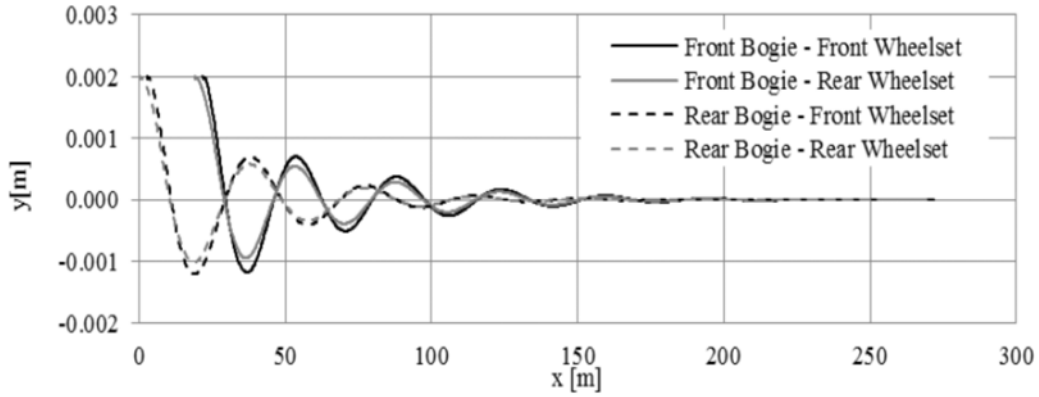

Figure 18. Wheelsets lateral displacement

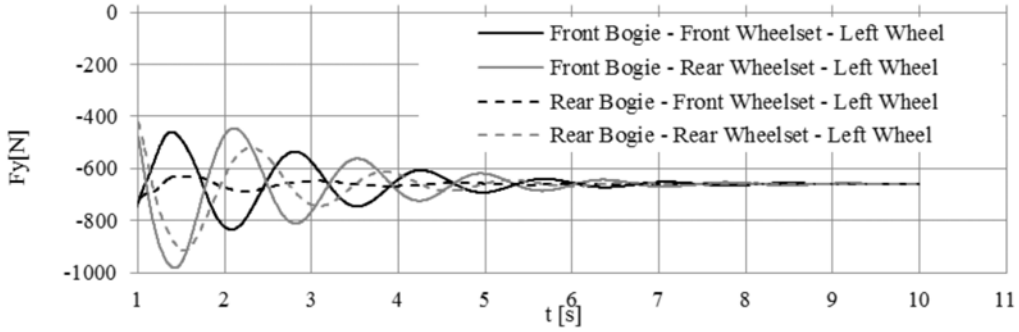

Figure 19. Lateral contact forces on the left wheels of the vehicle

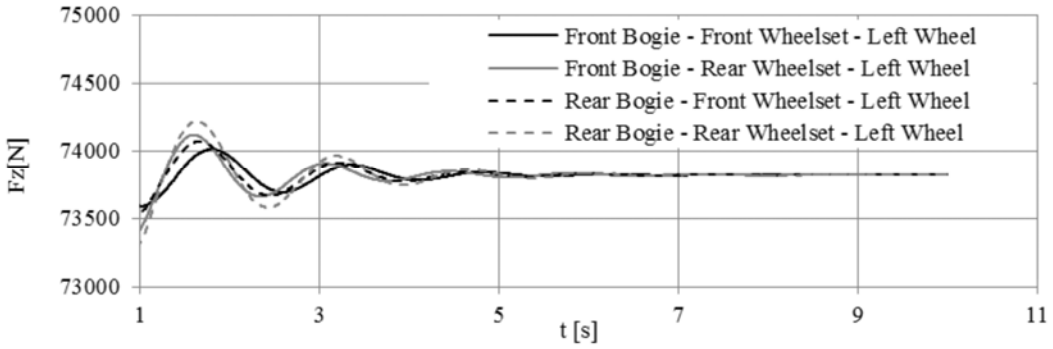

Figure 20. Vertical contact forces on the left wheels of the vehicle

10. Conclusions

The dynamic analysis of the loads imposed to the railway infrastructure by trainsets and, conversely, the damages on vehicles provoked by the track conditions has been attracting the attention of railway community in recent years. The raising interest on this subject has occurred mainly due to the development of new high-speed railway lines and to the common drive to upgrade the existing infrastructures. The increasing demands on railway transportation require improvements of the network capacity, which can be achieved either by increasing the speed of the traffic or by increasing the axle loads. However, both of these options place pressures on the existing infrastructures and the effects of these changes have to be carefully considered. The main goal of this work is to develop an advanced computational tool for railway dynamics, with innovative methodologies that are handled in a co-simulation environment, where all physical phenomena can be integrated. This includes not only the detailed representation of the vehicle, track and subgrade, but also the interaction among them. Such a tool can indicate solutions with technological relevance and give answer to the industry's most recent needs, contributing to improve the competitiveness of the railway transportation system. The results obtained show that the finite element methodology, proposed here to represent the track flexibility, is suitable for railway studies and it is quantitatively validated. Future developments of this work include the development of comparative studies in order to investigate the influence of track flexibility and of track conditions on vehicles performance. Also studies involving the consequences of trainset operation on railway infrastructure degradation are foreseen as future work. The establishment of partnerships with Portuguese railway operators and infrastructure manager gives good perspectives for the industrial application of the achievements of these studies.

Acknowledgments

The work reported here has been developed in the course of 2 national projects funded by FCT – Foundation for Science and Technology in which the authors have been involved, namely, the projects SMARTRACK, with the contract PTDC/EME-PME/101419/2008, and WEARWHEEL, with the contract PTDC/EME-PME/115491/2009.

References

[1] ERRAC, European Rail Research Advisory Council, Strategic Rail Research Agenda 2020, Brussels, Belgium, 2007.

[2] EC, European Commission, White Paper: Roadmap to a Single European Transport Area - Towards a Competitive and Resource Efficient Transport System, Brussels, Belgium, 2011.

[3] R.V. Dukkipati, and J.R. Amyot, Computer-Aided Simulation in Railway Dynamics, M. Dekker Inc., New York, New York, 1988.

[4] J. Pombo, J. Ambrósio, M. Pereira, R. Verardi, C. Ariaudo and N. Kuka, Influence of Track Conditions and Wheel Wear State on the Loads Imposed on the Infrastructure by Railway

Vehicles, *Computers and Structures*, 89, No. 21-22, (2011), pp. 1882-1894.

[5] P.E. Nikravesh, Computer-Aided Analysis of Mechanical Systems, Prentice-Hall, Englewood Cliffs, New Jersey, 1988.

[6] W. Schiehlen, Multibody Systems Handbook, Springer-Verlag, Berlin, Germany, 1990.

[7] A.A. Shabana, Dynamics of Multibody Systems, 2nd Edition, Cambridge University Press, Cambridge, United Kingdom, 1998.

[8] J.N. Reddy, An Introduction to the Finite Element Method, 3rd Edition, McGraw-Hill, 2005.

[9] O. Zienkiewicz and R. Taylor, The Finite Element Method, Butterwort-Heinemann, Woburn, Massachusetts, 2000.

[10] J. Pombo and J. Ambrósio, An Alternative Method to Include Track Irregularities in Railway Vehicle Dynamic Analyses, *Nonlinear Dynamics*, 68, (2012), pp. 161-176.

[11] J. Ambrósio, J. Pombo, M. Pereira, P. Antunes and A. Mósca, Recent Developments in Pantograph-Catenary Interaction Modelling and Analysis, *International Journal of Railway Technology*, 1, No. 1, (2012), pp. 249-278.

[12] J. Ambrósio, J. Pombo, M. Pereira, P. Antunes and A. Mósca, A Computational Procedure for the Dynamic Analysis of the Catenary-Pantograph Interaction in High-Speed Trains, *Journal of Theoretical and Applied Mechanics*, 50, No. 3, (2012), pp. 681-699.

[13] J. Pombo and J. Ambrósio, Application of a Wheel-Rail Contact Model to Railway Dynamics in Small Radius Curved Tracks, *Multibody Systems Dynamics*, 19, No. 1-2, (2008), pp. 91-114.

[14] J. Pombo, J. Ambrósio and M. Silva, A New Wheel-Rail Contact Model for Railway Dynamics, *Vehicle System Dynamics*, 45, No. 2, (2007), pp. 165-189.

[15] H.M. Lankarani and P.E. Nikravesh, A Contact Force Model with Hysteresis Damping for Impact Analysis of Multibody Systems, *AMSE Journal of Mechanical Design*, 112, (1990), pp. 369-376.

[16] H.M. Lankarani and P.E. Nikravesh, Continuous Contact Force Models for Impact Analysis in Multibody Systems, *Nonlinear Dynamics*, 5, (1994), pp. 193-207.

[17] J.J. Kalker, Simplified Theory of Rolling Contact, Progress Report Series C: Mechanical and Aeronautical Engineering and Shipbuilding, 1, pp. 1-10, Delft University of Technology, Delft, The Netherlands, 1973.

[18] Z.Y. Shen, J.K. Hedrick, and J.A. Elkins, A Comparison of Alternative Creep Force Models for Rail Vehicle Dynamic Analysis, *8th IAVSD Symposium on Dynamics of Vehicles on Road and Tracks*, (J. K. Hedrick, Ed.), Swets and Zeitlinger, Cambridge, Massachusetts, pp. 591-605, (1983).

[19] O. Polach, A Fast Wheel-Rail Forces Calculation Computer Code, *Vehicle System Dynamics*, Supplement 33, (1999), pp. 728-739.

[20] T. Hughes, The Finite Element Method: Linear Static and Dynamic Finite Element Analysis, Prentice-Hall, Englewood Cliffs, New Jersey, 1987.

[21] N. Newmark, A Method of Computation for Structural Dynamics, *ASCE Journal of the Engineering Mechanics Division*, 85, EM 3, (1959), pp. 67-94.

[22] J. Ambrósio, J. Pombo, F. Rauter and M. Pereira, A Memory Based Communication in the Co-Simulation of Multibody and Finite Element Codes for Pantograph-Catenary Interaction Simulation, *Multibody Dynamics*, (Bottasso C.L., Ed.), Springer, Dordrecht, The Netherlands, (2008), pp. 211-231.